Supplementary Information:

What External Perturbations Influence the Electronic Properties of Catalase Compound I?

Sam P. de Visser

The Manchester Interdisciplinary Biocenter and the School of Chemical Engineering and Analytical Science, 131 Princess Street, Manchester M1 7DN, UK.

Full reference 23: Gaussian 98, Revision A.7, Frisch, M. J.; Trucks, G. W.; Schlegel, H. B.; Scuseria, G. E.; Robb, M. A.; Cheeseman, J. R.; Zakrzewski, V. G.; Montgomery, Jr., J. A.; Stratmann, R. E.; Burant, J. C.; Dapprich, S.; Millam, J. M.; Daniels, A. D.; Kudin, K. N.; Strain, M. C.; Farkas, O.; Tomasi, J.; Barone, V.; Cossi, M.; Cammi, R.; Mennucci, B.; Pomelli, C.; Adamo, C.; Clifford, S.; Ochterski, J.; Petersson, G. A.; Ayala, P. Y.; Cui, Q.; Morokuma, K.; Malick, D. K.; Rabuck, A. D.; Raghavachari, K.; Foresman, J. B.; Cioslowski, J.; Ortiz, J. V.; Baboul, A. G.; Stefanov, B. B.; Liu, G.; Liashenko, A.; Piskorz, P.; Komaromi, I.; Gomperts, R.; Martin, R. L.; Fox, D. J.; Keith, T.; Al–Laham, M. A.; Peng, C. Y.; Nanayakkara, A.; Gonzalez, C.; Challacombe, M.; Gill,P. M. W.; Johnson, B.; Chen, W.; Wong, M. W.; Andres, J. L.; Gonzalez, C.; Head–Gordon, M.; Replogle, E. S.; Pople, J. A., Gaussian Inc., Pittsburgh, PA, 1998.

Table S1. Group spin densities and charges of optimized geometries of Cpd I & Cpd II of Catalase using Jaguar 5.5 at UB3LYP/LACVP level of theory.

	ρ_{Fe}	ρ_{O}	ρ_{Por}	ρ_{Tyr}	ρ_{Arg}	Q_{Fe}	Q_{O}	Q_{Por}	Q_{Tyr}	Q_{Arg}
$^4A_{2u}$	1.01	1.02	0.74	0.23	0.00	0.68	–0.27	0.10	–0.34	0.83
$^2A_{2u}$	1.10	0.99	–0.85	–0.24	0.00	0.68	–0.27	0.10	–0.34	0.83
$^2A_{1u}$	1.05	1.02	–1.03	–0.04	0.00	0.69	–0.27	0.22	–0.45	0.81
$^4A_{1u}$	1.06	1.01	0.93	0.00	0.00	0.69	–0.28	0.25	–0.47	0.81
$^6A_{2u}$	3.02	0.72	1.19	0.07	0.00	0.86	–0.29	0.00	–0.40	0.83
^{3}CpdII	1.10	0.97	–0.07	0.00	0.00	0.67	–0.30	–0.62	–0.52	0.77

Table S2. Single point UB3LYP/LACV3P+* calculations on UB3LYP/LACVP optimized geometries of Cpd I & Cpd II of Catalase using Jaguar 5.5.

	ρ_{Fe}	ρ_{O}	ρ_{Por}	ρ_{Tyr}	ρ_{Arg}	Q_{Fe}	Q_{O}	Q_{Por}	Q_{Tyr}	Q_{Arg}
$^4A_{2u}$	1.09	0.95	0.74	0.22	0.00	0.56	–0.17	0.00	–0.29	0.90
$^2A_{2u}$	1.20	0.92	–0.88	–0.24	0.00	0.63	–0.20	–0.02	–0.31	0.90
$^2A_{1u}$	1.14	0.96	–1.05	–0.05	0.00	0.60	–0.17	0.12	–0.42	0.87
$^4A_{1u}$	1.15	0.93	0.92	0.00	0.00	0.60	–0.19	0.17	–0.45	0.87
$^6A_{2u}$	3.15	0.64	1.16	0.05	0.00	0.65	–0.15	–0.06	0.06	0.50
^{3}CpdII	1.18	0.90	–0.07	–0.01	0.00	0.56	–0.20	–0.73	–0.48	0.85

Table S3. Single point calculations with ε = 5.7 on UB3LYP/LACVP optimized geometries of Cpd I & Cpd II of Catalase using Jaguar 5.5.

	ρ_{Fe}	ρ_{O}	ρ_{Por}	ρ_{Tyr}	ρ_{Arg}	Q_{Fe}	Q_{O}	Q_{Por}	Q_{Tyr}	Q_{Arg}
$^4A_{2u}$	1.08	0.95	0.74	0.22	0.01	0.67	–0.35	0.17	–0.34	0.85
$^2A_{2u}$	1.18	0.92	–0.86	–0.24	0.00	0.67	–0.36	0.18	–0.34	0.85
$^2A_{1u}$	1.11	0.96	–1.03	–0.04	0.00	0.69	–0.35	0.28	–0.45	0.83
$^4A_{1u}$	1.11	0.95	0.94	0.00	0.00	0.68	–0.35	0.32	–0.48	0.83
$^6A_{2u}$	3.04	0.68	1.22	0.06	0.00	0.84	–0.36	0.07	–0.40	0.85
^{3}CpdII	1.18	0.89	–0.07	0.00	0.00	0.66	–0.39	–0.56	–0.51	0.80

Table S4. Single point calculations with ε = 10.65 on UB3LYP/LACVP optimized geometries of Cpd I & Cpd II of Catalase using Jaguar 5.5.

	ρ_{Fe}	ρ_{O}	ρ_{Por}	ρ_{Tyr}	ρ_{Arg}	Q_{Fe}	Q_{O}	Q_{Por}	Q_{Tyr}	Q_{Arg}
$^4A_{2u}$	1.09	0.93	0.75	0.22	0.01	0.67	–0.37	0.18	–0.34	0.86
$^2A_{2u}$	1.19	0.90	–0.86	–0.23	0.00	0.67	–0.37	0.18	–0.34	0.86
$^2A_{1u}$	1.12	0.95	–1.03	–0.04	0.00	0.68	–0.36	0.30	–0.45	0.83
$^4A_{1u}$	1.13	0.93	0.94	0.00	0.00	0.68	–0.37	0.34	–0.48	0.83
$^6A_{2u}$	3.05	0.67	1.23	0.05	0.00	0.85	–0.38	0.08	–0.40	0.85
^{3}CpdII	1.21	0.86	–0.07	0.00	0.00	0.66	–0.41	–0.54	–0.51	0.80

Table S5. Group spin densities and charges of optimized geometries of Cpd I & Cpd II of Fe=O(Por)OH using Jaguar 5.5 at UB3LYP/LACVP level of theory.

	E [a]	ΔE [b]	ρ_{Fe}	ρ_{O}	ρ_{Por}	ρ_{OH}	Q_{Fe}	Q_{O}	Q_{Por}	Q_{OH}
$^4A_{2u}$	–1262.527096	0.00	0.98	1.08	0.58	0.36	0.58	–0.30	–0.09	–0.19
$^2A_{2u}$	–1262.526084	0.64	1.06	0.97	–0.62	–0.41	0.60	–0.30	–0.13	–0.17
$^4A_{1u}$	–1262.508585	11.62	1.00	1.00	0.91	0.09	0.53	–0.35	0.13	–0.31
$^2A_{1u}$	–1262.510076	10.68	1.00	1.01	0.90	0.09	0.53	–0.35	0.13	–0.31
^{3}CpdII	–1262.630828	–65.09 [c]	1.04	0.98	–0.10	0.08	0.50	–0.37	–0.80	–0.33

(a) in au. (b) in kcal mol^{-1}. (c) 65.09 kcal mol^{-1} = 2.82 eV.

Table S6. Single point UB3LYP/LACV3P+* calculations on UB3LYP/LACVP optimized geometries of Cpd I & Cpd II of Fe=O(Por)OH using Jaguar 5.5.

	E [a]	ΔE [b]	ρ_{Fe}	ρ_{O}	ρ_{Por}	ρ_{OH}	Q_{Fe}	Q_{O}	Q_{Por}	Q_{OH}
$^4A_{2u}$	–1263.106813	0.00	1.10	1.00	0.59	0.31	0.46	–0.20	–0.06	–0.20
$^2A_{2u}$	–1263.105742	0.67	1.18	0.89	–0.70	–0.37	0.48	–0.20	–0.11	–0.17
$^4A_{1u}$	–1263.095564	7.06	1.12	0.93	0.89	0.06	0.47	–0.26	0.09	–0.30
$^2A_{1u}$	–1263.096757	6.31	1.13	0.95	–1.15	0.07	0.47	–0.25	0.08	–0.30
^{3}CpdII	–1263.227621	–75.81 [c]	1.17	0.90	–0.12	0.05	0.52	–0.31	–0.86	–0.35

(a) in au. (b) in kcal mol^{-1}. (c) 75.81 kcal mol^{-1} = 3.29 eV.

Table S7. Single point calculations with ε = 5.7 on UB3LYP/LACVP optimized geometries of Cpd I & Cpd II of Fe=O(Por)OH using Jaguar 5.5.

	E_{solv} [a]	ΔE [a]	ρ_{Fe}	ρ_{O}	ρ_{Por}	ρ_{OH}	Q_{Fe}	Q_{O}	Q_{Por}	Q_{OH}
$^4A_{2u}$	–18.21	0.00	1.07	0.97	0.71	0.25	0.56	–0.39	0.10	–0.27
$^2A_{2u}$	–17.69	1.16	1.17	0.88	–0.77	–0.28	0.58	–0.40	0.07	–0.25
$^4A_{1u}$	–22.33	7.50	1.05	0.95	0.92	0.08	0.54	–0.42	0.23	–0.35
$^2A_{1u}$	–22.14	6.75	1.05	0.96	–1.10	0.09	0.54	–0.41	0.22	–0.35
^{3}CpdII	–54.25	–101.13 [b]	1.12	0.90	–0.09	0.07	0.51	–0.46	–0.67	–0.38

(a) in kcal mol^{-1}. (b) 101.13 kcal mol^{-1} = 4.39 eV.

Table S8. Single point calculations with ε = 10.65 on UB3LYP/LACVP optimized geometries of Cpd I & Cpd II of Fe=O(Por)OH using Jaguar 5.5.

	E_{solv} [a]	ΔE [a]	ρ_{Fe}	ρ_{O}	ρ_{Por}	ρ_{OH}	Q_{Fe}	Q_{O}	Q_{Por}	Q_{OH}
$^4A_{2u}$	–22.09	0.00	1.09	0.94	0.75	0.22	0.56	–0.42	0.15	–0.29
$^2A_{2u}$	–21.37	1.36	1.20	0.86	–0.82	–0.24	0.58	–0.42	0.11	–0.27
$^4A_{1u}$	–26.69	7.01	1.07	0.93	0.92	0.08	0.53	–0.43	0.26	–0.36
$^2A_{1u}$	–26.43	6.34	1.07	0.94	–1.09	0.08	0.53	–0.43	0.25	–0.35
^{3}CpdII	–62.43	–105.43 [b]	1.15	0.88	–0.10	0.07	0.51	–0.47	–0.66	–0.38

(a) in kcal mol^{-1}. (b) 105.43 kcal mol^{-1} = 4.57 eV.

Table S9. Group spin densities and charges of optimized geometries of Cpd I & Cpd II of Fe=O(Por)OSer using Jaguar 5.5 at UB3LYP/LACVP level of theory.

	E [a]	ΔE [b]	ρ_{Fe}	ρ_{O}	ρ_{Por}	ρ_{OH}	Q_{Fe}	Q_{O}	Q_{Por}	Q_{OH}
$^4A_{2u}$	–1584.955246	0.00	1.01	1.02	0.40	0.57	0.62	–0.29	–0.21	–0.12
$^2A_{2u}$	–1584.955144	0.06	1.07	0.98	–0.47	–0.58	0.63	–0.43	–0.11	–0.09
$^4A_{1u}$	–1584.935473	12.41	1.02	0.99	0.91	0.08	0.57	–0.34	0.15	–0.38
$^2A_{1u}$	–1584.937152	11.35	1.02	1.00	–1.08	0.06	0.57	–0.33	0.13	–0.37
^{3}CpdII	–1585.061207	–66.49 [c]	1.07	0.96	–0.09	0.06	0.55	–0.36	–0.75	–0.44

(a) in au. (b) in kcal mol^{-1}. (c) –66.49 kcal mol^{-1} = 2.88 eV.

Table S10. Single point UB3LYP/LACV3P+* calculations on UB3LYP/LACVP optimized geometries of Cpd I & Cpd II of Fe=O(Por)OSer using Jaguar 5.5.

	E [a]	ΔE [b]	ρ_{Fe}	ρ_{O}	ρ_{Por}	ρ_{OH}	Q_{Fe}	Q_{O}	Q_{Por}	Q_{OH}
$^4A_{2u}$	–1585.733703	0.00	1.09	0.96	0.41	0.54	0.49	–0.16	–0.29	–0.04
$^2A_{2u}$	–1585.733577	0.08	1.16	0.92	–0.49	–0.59	0.50	–0.16	–0.33	–0.01
$^4A_{1u}$	–1585.721692	7.54	1.12	0.93	0.88	0.07	0.40	–0.21	0.11	–0.30
$^2A_{1u}$	–1585.722979	6.73	1.12	0.94	–1.10	0.04	0.39	–0.20	0.10	–0.29
^{3}CpdII	–1585.857814	–77.88 [c]	1.16	0.90	–0.11	0.05	0.41	–0.25	–0.80	–0.36

(a) in au. (b) in kcal mol^{-1}. (c) 77.88 kcal mol^{-1} = 3.38 eV.

Table S11. Single point calculations with ε = 5.7 on UB3LYP/LACVP optimized geometries of Cpd I & Cpd II of Fe=O(Por)OSer using Jaguar 5.5.

	E_{solv} [a]	ΔE [a]	ρ_{Fe}	ρ_{O}	ρ_{Por}	ρ_{OH}	Q_{Fe}	Q_{O}	Q_{Por}	Q_{OH}
$^4A_{2u}$	–22.48	0.00	1.07	0.95	0.43	0.55	0.62	–0.37	–0.12	–0.13
$^2A_{2u}$	–22.27	0.27	1.15	0.91	–0.46	–0.60	0.62	–0.37	–0.15	–0.10
$^4A_{1u}$	–26.29	8.61	1.08	0.93	0.90	0.09	0.57	–0.42	0.21	–0.36
$^2A_{1u}$	–25.72	8.12	1.07	0.94	–1.07	0.06	0.57	–0.41	0.20	–0.36
^{3}CpdII	–53.48	–97.49 [b]								

(a) in kcal mol^{-1}. (b) –97.49 kcal mol^{-1} = 4.23 eV.

Table S12. Single point calculations with ε = 10.65 on UB3LYP/LACVP optimized geometries of Cpd I & Cpd II of Fe=O(Por)OSer using Jaguar 5.5.

	E_{solv} [a]	ΔE [a]	ρ_{Fe}	ρ_{O}	ρ_{Por}	ρ_{OH}	Q_{Fe}	Q_{O}	Q_{Por}	Q_{OH}
$^4A_{2u}$	–26.48	0.00	1.09	0.93	0.43	0.55	0.61	–0.39	–0.09	–0.13
$^2A_{2u}$	–26.33	0.21	1.17	0.90	–0.47	–0.60	0.62	–0.39	–0.13	–0.10
$^4A_{1u}$	–30.71	8.18	1.09	0.91	0.91	0.09	0.57	–0.43	0.23	–0.37
$^2A_{1u}$	–30.32	7.52	1.08	0.93	–1.07	0.06	0.57	–0.42	0.21	–0.36
^{3}CpdII	–61.60	–101.61 [b]								

(a) in kcal mol^{-1}. (b) –101.61 kcal mol^{-1} = 4.41 eV.

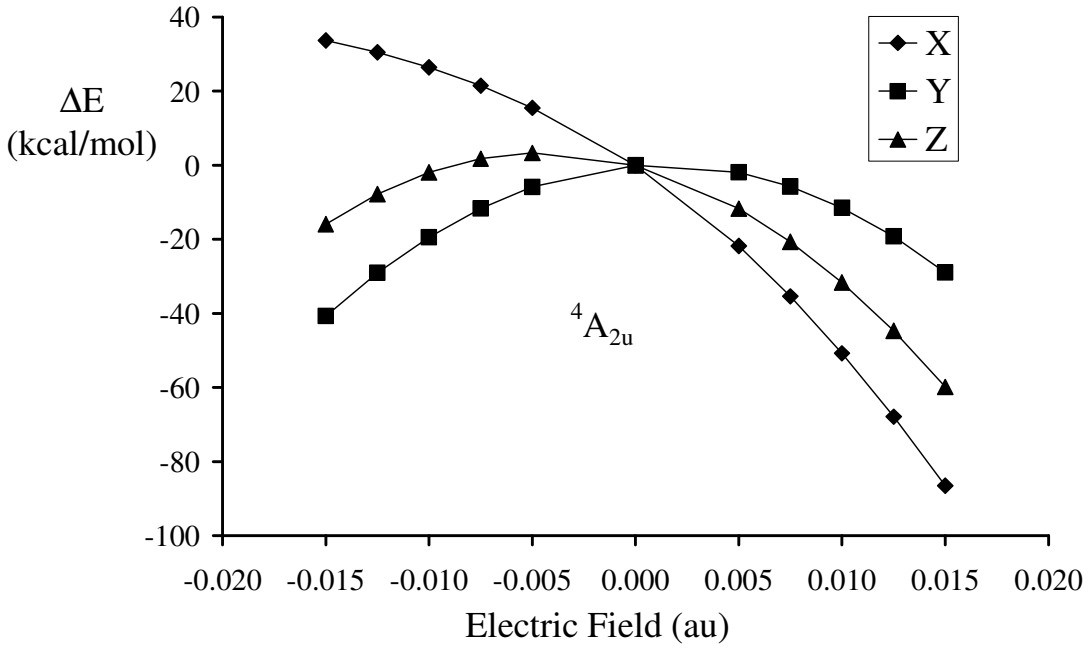

Figure S1. Relative energies of the lowest lying quartet spin state with the addition of an electric field along the molecular *x*–, *y*–, or *z*–axis (as defined in Figure 4 of the main text). All energies are in kcal mol^{-1} with respect of the unperturbed system.

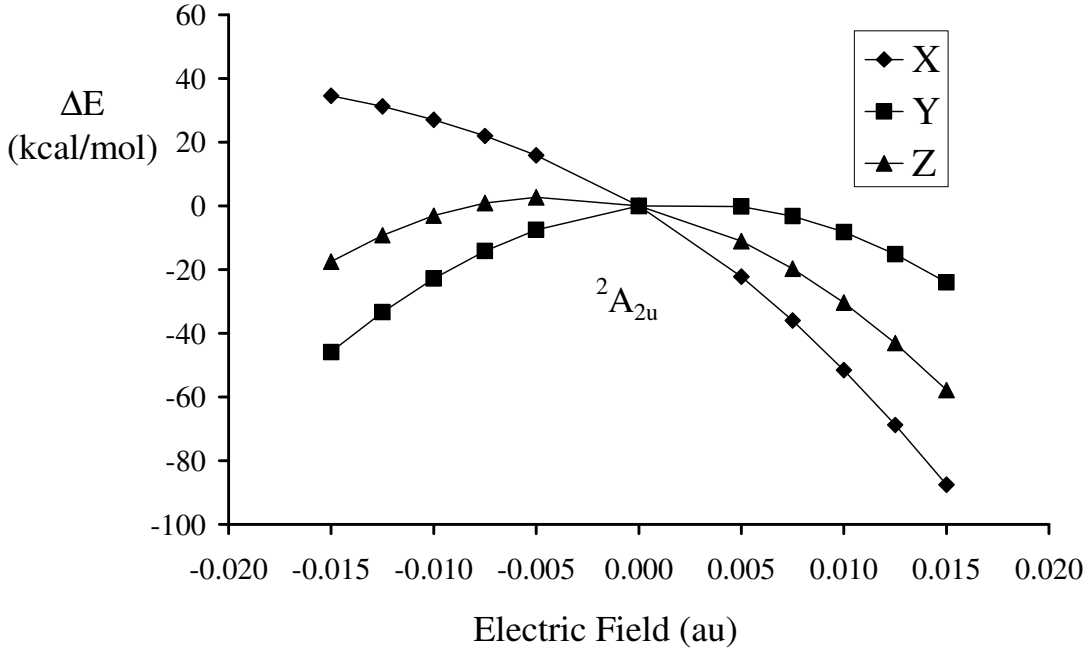

Figure S2. Relative energies of the lowest lying doublet spin state with the addition of an electric field along the molecular *x*–, *y*–, or *z*–axis (as defined in Figure 4 of the main text). All energies are in kcal mol^{-1} with respect of the unperturbed system.

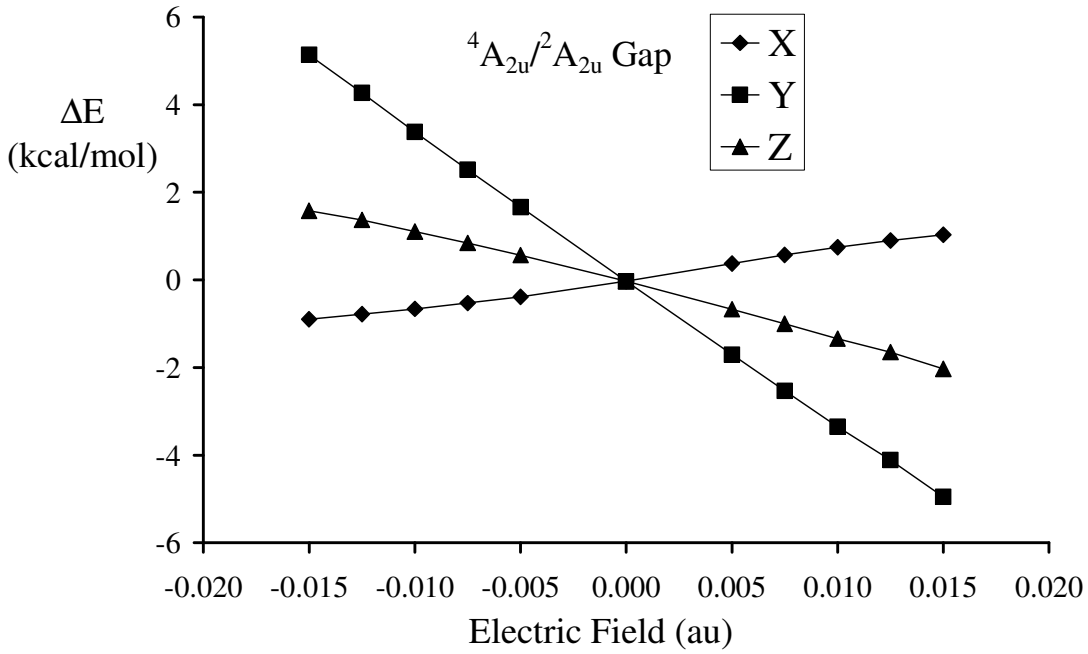

Figure S3. Quartet–doublet energy gap under the influence of an electric field along the molecular *x*–, *y*–, or *z*–axis (as defined in Figure 4 of the main text). A positive value denotes a quartet ground state; all energies are in kcal mol^{-1}.

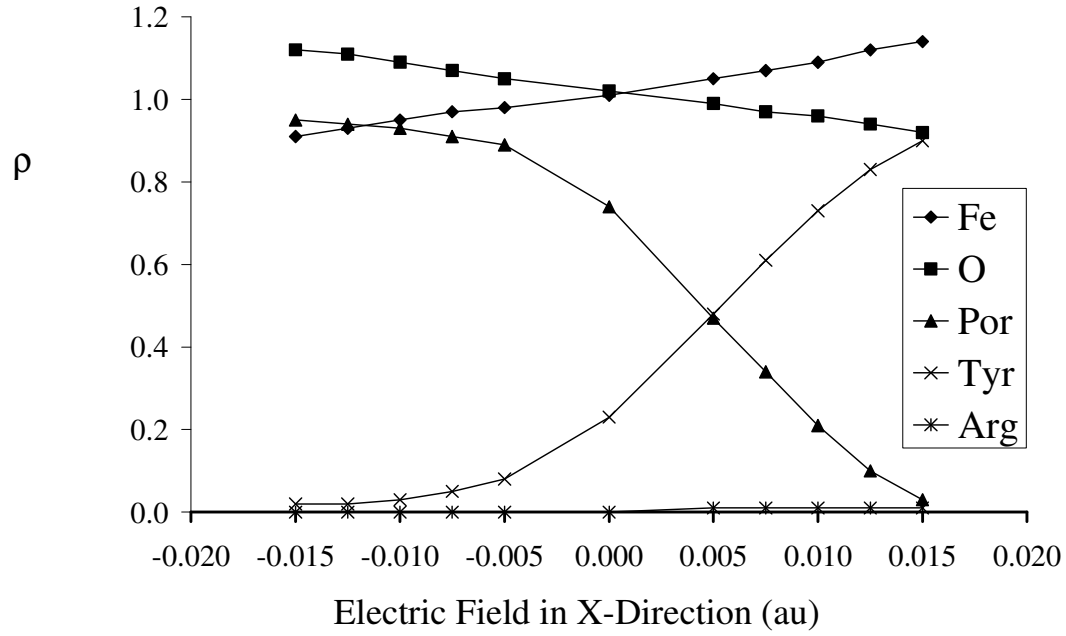

Figure S4. Group spin density changes of the lowest lying quartet spin state under the influence of an electric field along the molecular *x*–axis (as defined in Figure 4 of the main text).

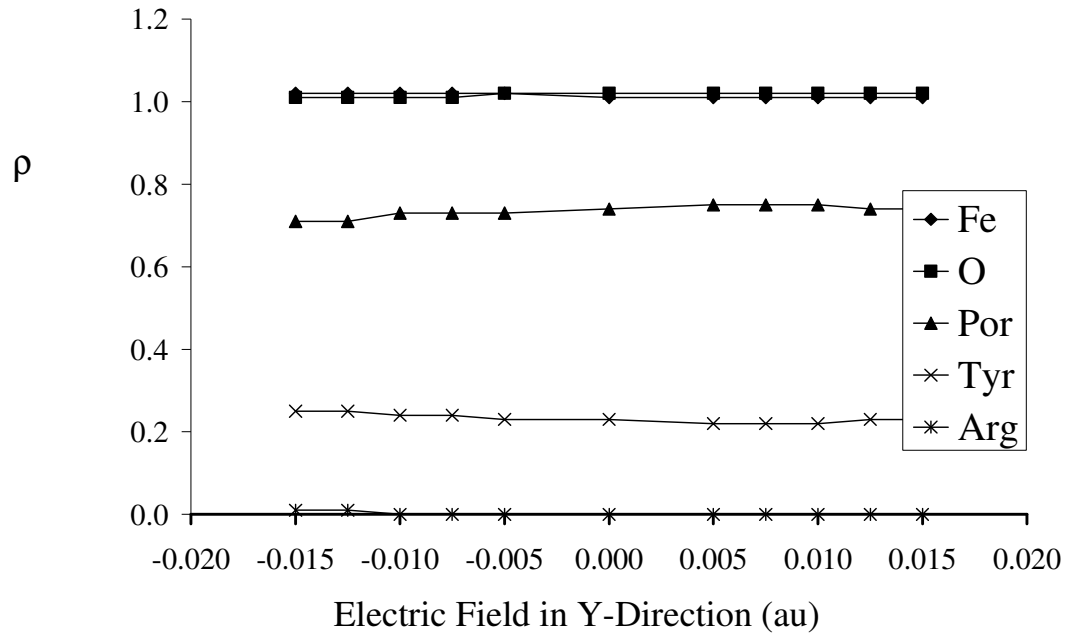

Figure S5. Group spin density changes of the lowest lying quartet state under the influence of an electric field along the molecular *y*–axis (as defined in Figure 4 of the main text).

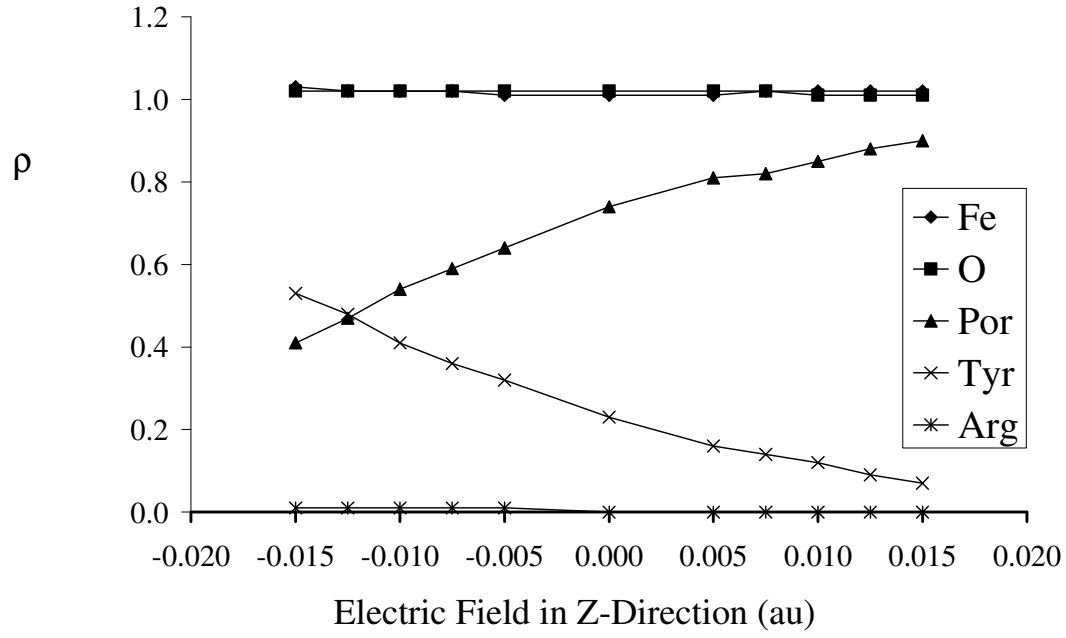

Figure S6. Group spin density changes of the lowest lying quartet spin state under the influence of an electric field along the molecular *z*–axis (as defined in Figure 4 of the main text).

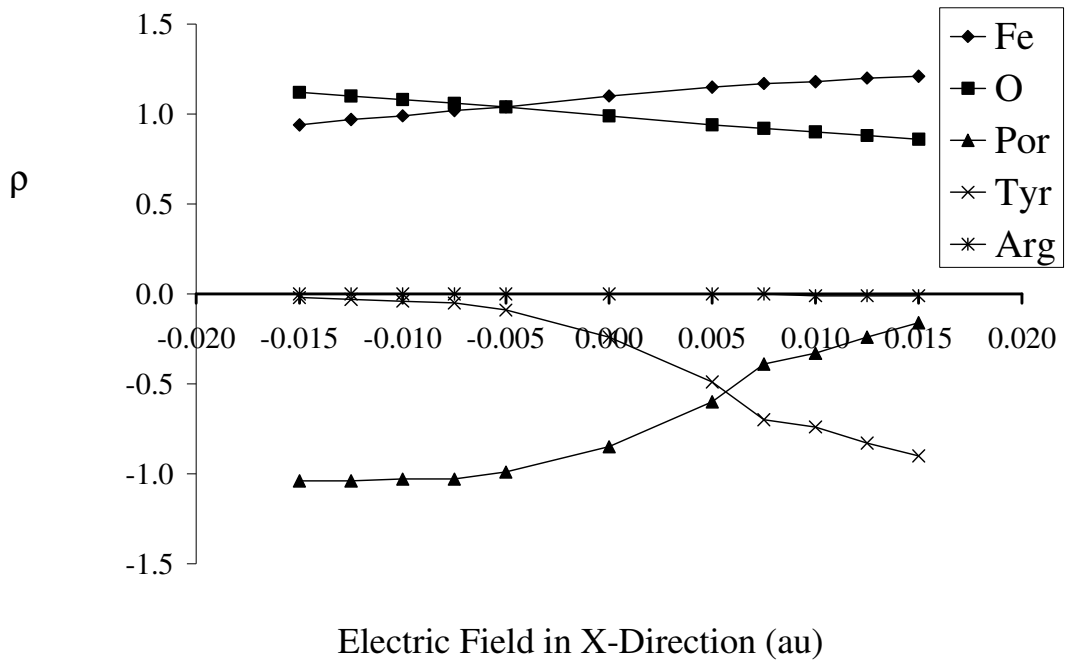

Figure S7. Group spin density changes of the lowest lying doublet spin state under the influence of an electric field along the molecular *x*–axis (as defined in Figure 4 of the main text).

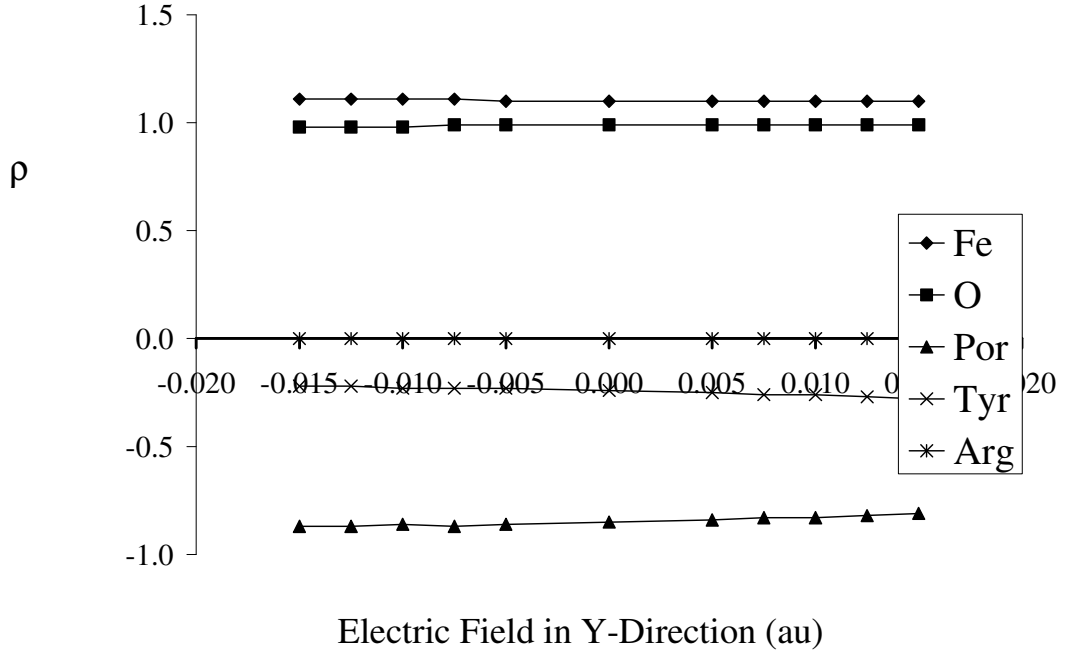

Figure S8. Group spin density changes of the lowest lying doublet spin state under the influence of an electric field along the molecular *y*–axis (as defined in Figure 4 of the main text).

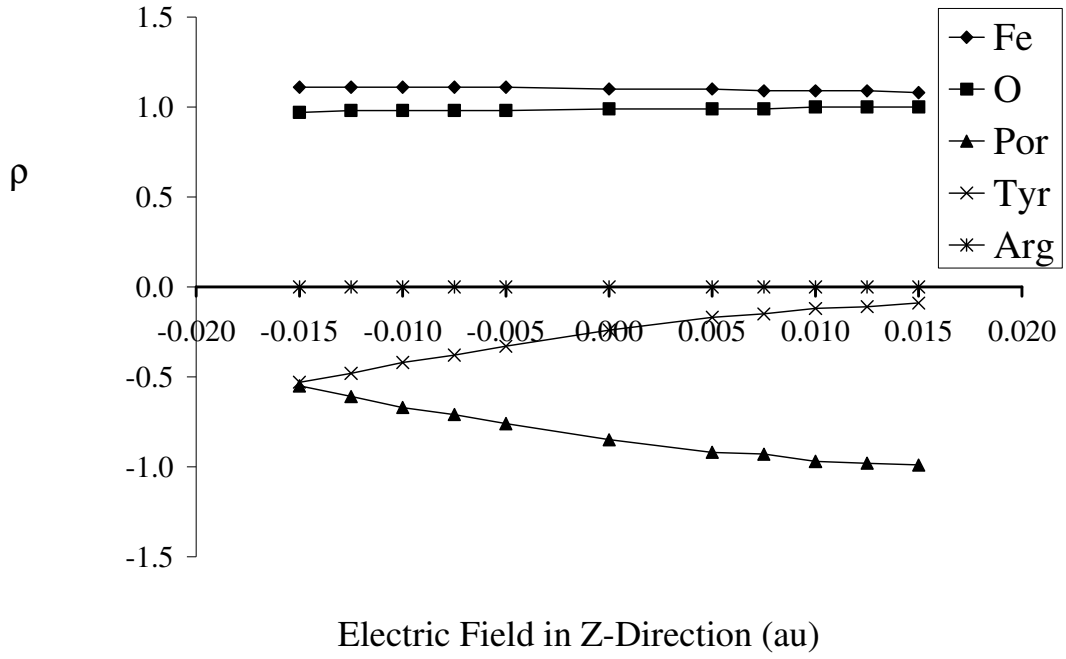

Figure S9. Group spin density changes of the lowest lying doublet spin state under the influence of an electric field along the molecular *z*–axis (as defined in Figure 4 of the main text).